RESEARCH ARTICLE

Rising mean and extreme near-surface air temperature across Nepal

Ramchandra Karki[1,2] | Shabeh ul Hasson[1,3] | Lars Gerlitz[4] |
Rocky Talchabhadel[2,5] | Udo Schickhoff[1] | Thomas Scholten[6] | Jürgen Böhner[1]

[1]Center for Earth System Research and Sustainability, Institute of Geography, University of Hamburg, Hamburg, Germany

[2]Department of Hydrology and Meteorology, Government of Nepal, Kathmandu, Nepal

[3]Department of Space Science, Institute of Space Technology, Islamabad, Pakistan

[4]Section Hydrology, GFZ German Research Centre for Geosciences, Potsdam, Germany

[5]Disaster Prevention Research Institute, Kyoto University, Kyoto, Japan

[6]Department of Geosciences, Soil Science and Geomorphology, University of Tübingen, Tübingen, Germany

Correspondence
Jürgen Böhner, Center for Earth System Research and Sustainability, Institute of Geography, University of Hamburg, Bundesstraße 55, 20146 Hamburg, Germany.
Email: juergen.boehner@uni-hamburg.de

Abstract

Owing to unique topographic and ecological diversity, central Himalayan state of Nepal is exposed to adverse impacts of climate change and associated disasters. However, countrywide historical assessment of mean and extreme temperature changes, a prerequisite for devising adequate adaptation strategies, is still lacking. Here, we present a comprehensive picture of mean and extreme temperature trends across Nepal over the 1980–2016 period, based on high-quality daily temperature observations from 46 stations. Our results suggest that besides winter cooling in southern lowlands, the country features a widespread warming, which is higher for maximum temperature (~0.04°C·year^{-1}) than for minimum temperature (~0.02°C·year^{-1}), over the mountainous region than in valleys and lowlands and during the pre-monsoon season than for the rest of the year. Consistently, we found a higher increasing trend for warm days (13 days·decade^{-1}) than for warm nights (4 days·decade^{-1}), whereas the rates of decrease for cold days and cold nights are the same (6 days·decade^{-1}). Further investigations reveal that pronounced warming in maximum temperature over mountain regions can be attributed to less cloud cover and snowfall in recent decades during non-monsoon seasons as a result of positive geopotential height anomalies and strengthening of anticyclonic circulations in the mid-to-upper troposphere. Similarly, increased stability of lower atmosphere during winter and post-monsoon seasons caused prolonged and frequent periods of fog over lowlands, resulting in significant winter cooling there.

KEYWORDS
adaptation, climate change, climatic extremes, Himalayas, increase in warm days and nights, Nepal

1 | INTRODUCTION

Mean global near-surface air temperature has increased by 0.85°C over the period 1880–2012, and the decade of the 2000s has been the warmest on record (IPCC, 2013). Simultaneously, extreme weather and climate events have increasingly become more frequent and more intense globally. This has led to higher risk of climate-induced disasters (e.g., warm spells, heat and cold waves, and droughts and floods) and an increased exposure of the society, economy, and ecosystems to climate change impacts in recent decades. As severity of these disasters vary temporally and spatially, an assessment of changes in

climate extremes at local scale is an urgent requirement, particularly for the development of adaptation strategies.

Consistent with the global pattern, South Asia has experienced a general increase in mean and extreme near-surface air temperatures (hereinafter temperature), and such extremes are anticipated to be more frequent in future (Sivakumar and Stefanski, 2011). However, temperature trend characteristics vary depending on the season, region, and temperature variable (maximum or minimum). For instance, the greater Himalayan region of Pakistan (north of 35°N latitude) exhibits a summer cooling and a decrease in warm nights (Sheikh et al., 2015; Hasson et al., 2017), which contrasts with the general warming trend (Klein Tank et al., 2006; Caesar et al., 2011; Sheikh et al., 2015). Likewise, prominent increase observed in maximum temperature over central and western Himalayan mountains (Shrestha et al., 1999; Bhutiyani et al., 2007; Kattel and Yao, 2013; Nayava et al., 2017) is in direct contrast to prominent increase observed in minimum temperatures over South Asia, India, China, and Tibet in recent decades (Alexander et al., 2006; Klein Tank et al., 2006; Panda et al., 2014; Ding et al., 2018; Tong et al., 2019). Furthermore, dependencies of extreme temperature trends with elevation and latitude have been noted in the region over the period 1971–2000 (Revadekar et al., 2013). In general, spatially consistent warming trends were found for low elevations and latitudes. However, for high elevations and latitudes, a mixed trend featuring both warming and cooling in different seasons is evident. These spatially varying trend characteristics within the Himalayan mountains indicate a strong control of local-scale terrain features on climatic trends, stressing on the need of a comprehensive assessment at the local scale (Shrestha et al., 1999; Bhutiyani et al., 2007; Shrestha et al., 2012; Hasson et al., 2016; Mainali and Pricope, 2017; Sheikh et al., 2015; Hasson et al., 2018).

The spatial focus of our study is the central Himalayan region of Nepal (Figure 1), where a significantly higher rate of warming has been observed relative to the Western Himalaya (Shrestha et al., 1999; Sheikh et al., 2015). Owing to varying climatic and ecological conditions, the country is already exposed to cold and warm temperature extremes and related disasters, in addition to its high vulnerability to climate change impacts. Thus, the local-scale investigation of temperature trends is essential for impact assessments for different societal end economic sectors and for the development of effective management strategies in order to adapt and mitigate the disasters and ensuring wellbeing of rural mountain communities. However, despite high importance, studies on mean and extreme temperature are limited in Nepal (Table 1).

For instance, analysing observed trends across Nepal, Shrestha et al. (1999) found an average annual warming of 0.06°C·year^{-1} between 1971 and 1994, with a more pronounced increase at high-elevation areas. In contrast to those findings, Nayava et al. (2017) reported the highest warming at the Himalayan hills between the elevation range of 1,000 and 2,000 m above sea level (m asl) and lower warming over lowlands and high mountains for the 1981–2010 period. A few studies focusing on smaller regions and recent decades reveal regional disparities for different parts of Nepal (Qi et al., 2013; Salerno et al., 2015; Khatiwada et al., 2016; Shrestha et al., 2017). Compared with the national-level study (Shrestha et al., 1999), which shows the highest warming in post-monsoon, basin-level studies (for Koshi and Karnali basins), indicate highest warming rates in pre-monsoon (Salerno et al., 2015; Khatiwada et al., 2016). These varying trend features may likely be due to differences in analysed periods, stations utilized, and the studied regions. For analysis of extremes, Baidya et al. (2008) analysed changes in temperature extremes for the 1971–2006 period across Nepal based on eight stations. They found an increase of warm temperature extreme indices and a decrease of cold extremes, a pattern consistent to regional studies (Klein Tank et al., 2006; Caesar et al., 2011; Sheikh et al., 2015). However, the low number of

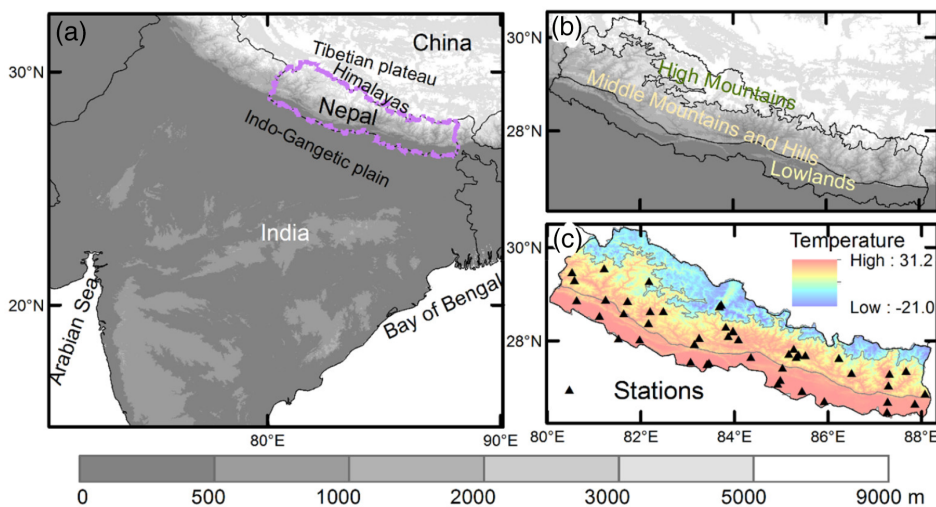**FIGURE 1** (a) Location of Nepal. Political boundary is shown by magenta polygon. Topography is shaded in grey, (b) three broad physiographic regions of Nepal, such as, lowlands, middle mountains and hills, and high mountains are shown in polylines and the terrain in shaded in grey, and (c) mean annual normal maximum temperature (°C) and location of 46 stations used in this study [Colour figure can be viewed at wileyonlinelibrary.com]

TABLE 1 Overview of mean and extreme temperature studies in Nepal and number of temperature stations from Nepal used in those studies

Study	Region	Period	Method	Stations	Trends
Shrestha *et al.* (1999)	Nepal	1971–1994	MK, OLSR	49	Mean
Baidya *et al.* (2008)	Nepal	1971–2006	ETCCDI, OLSR	8	Mean and extremes
Nayava *et al.* (2017)	Nepal	1981–2010	OLSR	21	Mean
Kattel and Yao (2013)	Mountains of Nepal	1980–2009	MK, OLSR	13	Mean
Shrestha *et al.* (2017)	Koshi river basin	1975–2010	ETCCDI, OLSR	11	Mean and extremes
Qi *et al.* (2013)	Koshi river basin	1971–2009	MK, SS	10	Mean
Khatiwada *et al.*(2016)	Karnali river basin	1981–2012	MK, SS	7	Mean
Salerno *et al.* (2015)	Koshi river basin	1994–2012	MK, SS	11	Mean
Sheikh *et al.* (2015)	South Asia	1971–2000	ETCCDI, OLSR	20	Mean and extremes
Revadekar *et al.* (2013)	South Asia	1971–2000	ETCCDI, OLSR	6	Extremes
Caesar *et al.* (2011)	Indo-pacific	1971–2005	ETCCDI, OLSR	7	Mean and extremes
Karki *et al.* (2018)	Nepal (this study)	1980–2016	ETCCDI, MK, SS	46	Mean and extremes

Abbreviations: ETCCDI, different temperature indices defined from expert team; OLSR, ordinary least square regression; SS, Sen's slope.

stations are not sufficient to draw a countrywide picture of extreme temperature trends in the complex terrain and varying climatic zones. From a comprehensive list of temperature-related studies over Nepal given in Table 1, it is obvious that a countrywide picture of temperature trends for recent decades is still missing, particularly for temperature extremes.

Complementing findings of previous studies, this study presents a comprehensive picture of mean and extreme temperature trends across Nepal, using high-quality daily temperature observations from 46 long-term climatic stations covering the period of 1980–2016. The analysis based on an extended number of high-quality station data up to recent years for the study area aims at a spatially and temporally complete investigation of temperature trends. We have derived 12 extreme temperature indices from daily data for individual stations as recommended by the World Meteorological Organization Expert Team on Climate Change Detection and Indices (ETCCDI). Trends in mean seasonal temperatures and annual temperature extreme indices are assessed using the Sen slope method (Sen, 1968), whereas the significance of trends is assessed using a robust nonparametric Mann−Kendall (MK) trend test (Mann, 1945; Kendall, 1975) in combination with a trend-free prewhitening (TFPW) procedure (Yue *et al.*, 2003). Subsequently, the trend characteristics in different topoclimatic environments are examined. In addition, possible influence of change in circulation features and cloud cover variations on the observed temperature changes is explored using the ERA-Interim reanalysis dataset (Dee *et al.*, 2011).

2 | STUDY AREA

Nepal is characterized by unique topographic and physiographic features as it is lying along the southern slopes of the Central Himalayan between 26.36°–30.45°N and 80.06°–88.2°E, covering an area of 147,181 km^2 (Figure 1). Topography varies between 60 m asl in southern lowlands and 8,848 m asl in the northern within shorter than 200 km latitudinal extent of the country (Figure 1b). Following the topographic gradient, the country is divided into five standard physiographic regions, such as Terai, Siwaliks, middle mountains, high mountains, and high Himalaya, which can further be grouped into three broader zones, namely, lowlands (Terai and Siwaliks, commonly known as flat plains), mid-mountains and hills, and high mountains (Himalayas; Duncan and Biggs, 2012; Miehe *et al.*, 2015). Owing to unique topographic and physiographic gradients, Nepal features diverse climatic conditions that vary from tropical in the southern lowlands to polar in the high mountains (Karki *et al.*, 2016). Nepal's high mountains are covered with snow and glaciers, whereas lowlands and mid-mountains and hills contain mostly forest and agriculture land (Uddin *et al.*, 2015).

Nepal has four main seasons, such as, post-monsoon (October–November), winter (December–February), pre-monsoon (March–May), and monsoon (June–September). Dry and cold westerly winds in the upper troposphere influence the study area during non-monsoon months, whereas monsoon season is characterized by warm and moist southerly to south-easterly near-surface flow conditions (Böhner and Lehmkuhl, 2006; Hasson *et al.*, 2014; Gerlitz *et al.*, 2015; Hasson, 2016; Kadel *et al.*, 2018). Post-monsoon is the driest season with mainly clear sky conditions, whereas winter is the coldest season. During winter, western disturbances bring precipitation, which mainly falls as snow at high elevations, with peak around 5,000 m asl (Lang and Barros, 2004; Böhner *et al.*, 2015). Pre-monsoon features highest solar radiation, warmest temperatures, and occasional localized convective precipitation. The majority of

precipitation occurs during the monsoon season, which accounts for more than 80% of the annual precipitation (Shrestha, 2000; Karki *et al.*, 2017a). Generally, peak annual and monsoon precipitation is observed between 2,000 and 3,500 m asl elevation at the windward Himalayan slopes, whereas very high elevations and north facing leeward slopes receive little precipitation (Böhner *et al.*, 2015; Talchabhadel *et al.*, 2018). Owing to topography, extreme temperature differences between the southern lowlands and the high mountains are evident within a short horizontal distance. Highest temperatures are observed over the lowlands and high mountains in May and June, respectively, where the highest maximum temperature exceeds 45°C over the southern lowlands (Shrestha and Aryal, 2011). Lowest temperatures are observed during December or January, whereas high mountain regions above 5,000 m asl features sub-zero mean daily temperature throughout the year (Karki *et al.*, 2017b). For example, mean daily temperatures observed at the southern slopes of Mt. Everest (at an elevation of 8,000 m asl.) is as low as −42°C (Gerlitz, 2014).

3 | DATA AND METHODOLOGY

3.1 | Data

We used the daily maximum temperature (T_{max}) and daily minimum temperature (T_{min}) observations from a full set of long-term climatic stations of the Department of Hydrology and Meteorology (DHM), Nepal. As observations within the entire network are taken with the same type of mercury (alcohol) containing thermometers for maximum and minimum temperatures at 1.25–2 m above the surface, data homogeneity is ensured in terms of the measurement method. In the DHM database, the longest record goes back to 1953. Later, the number of stations was increased to around 8, 39, 64, 97, and 140 in the year 1960, 1970, 1980, 1990, and at present, respectively. As continuous data were not available from all the stations due to either short-term discontinuity or relocation, we have restricted our analysis to recent period keeping in view the maximum number of stations with good spatial coverage across Nepal. A maximum number of high-quality data stations with continuous data records and good spatial coverage across the county was available for the period 1980–2016. For each year within this period, if more than 20% of the daily values were missing, we considered the whole year as missing (WMO, 2010). Similarly, stations with 20% missing years were excluded to ensure completeness of the data. As non-climatic factors, such as, change in measurement methods and observational practice, the aggregation method, or a change of the station location and exposure often cause data quality issues and

sudden shifts in the time series, all records are investigated for quality and homogeneity using the RClimDexV1.1 and RHTestsV4 toolkit developed by the ETCCDI. This software is open source and described in detail on the ETCCDI homepage (http://etccdi.pacificclimate.org/software.shtml).

RClimDex identifies the potential outliers and erroneous daily maximum (T_{max}) and minimum temperature (T_{min}) values. Errors of T_{min} higher or equal to T_{max} and outliers, identified as value outside 4 *SD* (4σ) from mean as employed in Shrestha *et al.* (2017), were manually checked for potential faults, such as mixing up T_{min} and T_{max}, and other typing errors during digitization. All confirmed erroneous values were subsequently replaced as missing values.

Homogenization of climatic data from the mountainous regions is challenging. Although, relative homogeneity testing is recommended, however, it is often not possible due to unavailability of homogenous reference time series. The RHTests software package can test the homogeneity without the reference time series and has demonstrated comparable level of performance to other homogeneity test methods (Caesar *et al.*, 2011). It compares the goodness of fit of a two-phase regression model with that of a linear trend for the entire time series to identify a step change (Wang, 2008). For each participating stations, we have examined the homogeneity of mean monthly maximum and mean monthly minimum temperatures separately, without a reference time series.

Few stations with shifts in both T_{max} and T_{min} were excluded and we did not attempt to adjust the time series based on homogeneity test. Although some suspicious stations passed the homogeneity test for either T_{max} or T_{min}, we excluded them from further analysis based on their known history of change (personal communication with local observers and sparsely available metadata in DHM record). Examples are the Dhankuta and Gorkha stations, which were shifted to lower elevations. Likewise, Dipayal Doti, Butwal, and Palpa stations have been frequently shifted from their original locations. Few additional stations, such as, Simari, Panipokhari, and Ranijaruwa with known poor data quality in recent years (first author's field visits and data analysis at DHM) were also excluded from the analysis. For around 15 stations, we found shifts in either T_{max} or T_{min}. The best station of Kathmandu Airport also features a shift in 1998 for T_{min} even though there was no change in the instrument or location. Most of the stations show strong positive temperature anomalies in T_{max} after 1997. It is possible that the shifts indicate natural climatic variability as was noted by Caesar *et al.* (2011). The confirmation can be possible when further stations information will be available from DHM in near future. After sorting for completeness, quality, and homogeneity, the observations were available only from 46 stations for final analysis (Supporting Information Table S1 and Figure 1c). Around 23 stations from the middle

mountains and hills, and the lowlands of Nepal feature no missing values.

In order to investigate possible drivers and the mechanism of warming and cooling over Nepal, we have used the ERA-Interim reanalysis dataset available at 0.75° horizontal resolution (Dee *et al.*, 2011). In general, the ERA-Interim captures the seasonal and spatial variations of temperature trends in Nepal and thus is considered as a valuable dataset for investigation of relevant large-scale atmospheric processes (Supporting Information Figure S1).

3.2 | Methodology

3.2.1 | Means and extreme indices

Mean seasonal maximum and minimum temperatures were computed from the daily observations from 46 stations for four main seasons of post-monsoon (October–November), winter (December–February), pre-monsoon (March–May), and monsoon (June–September). From the same daily dataset, we have computed 12 extreme temperature indices that are recommended by the ETCCDI (http://etccdi.pacificclimate.org/; Table 2) using RClimDexV1.1. These indices can be divided into three groups: (a) absolute indices; (b) threshold- and duration-based indices, and; (c) percentile-based indices. The absolute indices are the hottest day (TXx), warmest night (TNx), coldest day (TXn), and coldest night (TNn). The duration and threshold indices are summer days (SU25), WSDI (warm spell duration indicator), tropical nights (TR20), and cool days (ID15). As cold spell duration indicator featured no trend in most of the stations, we did not present it in this study. Percentile-based temperature indices account for the spatial variation of temperature and may better represent the spatial aspects of temperature extremes than other indices. Cool nights

(days) are calculated as the annual number of days with minimum (maximum) temperatures lower than the 10th percentile value of the entire record. Warm nights (days) correspond to the number of days that are warmer than the 90th percentile value. The 90th and 10th percentiles reference values for stations are considered from the 30-year base period of 1981–2010.

3.2.2 | Trend estimation and significance

We used the nonparametric MK (Mann, 1945; Kendall, 1975) test to investigate the significance of trends of annual extreme temperature indices and mean seasonal temperature time series. The MK test has been extensively used to assess the significance of monotonic trends in hydrometeorological time series and has been explained in detail in several studies (Hasson *et al.*, 2017; Karki *et al.*, 2017a; Talchabhadel *et al.*, 2018). Although the test is independent of the distribution and can cope with missing data and outliers, the presence of autocorrelation can affect the MK test results (Yue and Wang, 2002; Yue *et al.*, 2003). To address this issue, we use the TFPW method proposed by Yue *et al.* (2003). In the TFPW approach, first a true magnitude of a linear trend is estimated using the method proposed by Sen (1968), a nonparametric method that can cope with missing value and outliers. The estimated true trend magnitude is then removed from the original time series and the lag-1 autocorrelation is subsequently estimated and removed, if necessary, from the detrended time series. The real magnitude of trend is added back to the serially independent time series (detrended time series with no significant autocorrelation). Finally, the MK test is applied in order to detect the statistical significance of trends, in our case, based on a 5% significance level.

TABLE 2 The extreme temperature indices included in this study

Indices category	ID	Indicator name	Definitions	Units
Absolute	TXx	Hottest day	Annual maximum value of daily maximum temp	°C
	TNx	Warmest night	Annual maximum value of daily minimum temp	°C
	TXn	Coldest day	Annual minimum value of daily maximum temp	°C
	TNn	Coldest night	Annual minimum value of daily minimum temp	°C
Percentile	TN10p	Cool nights	Percentage of days when TN < 10th percentile	%
	TX10p	Cool days	Percentage of days when TX < 10th percentile	%
	TN90p	Warm nights	Percentage of days when TN > 90th percentile	%
	TX90p	Warm days	Percentage of days when TX > 90th percentile	%
Duration and fixed threshold	SU25	Summer days	Annual count when TX (daily maximum) > 25°C	days
	WSDI	Warm spell duration indicator	Annual count of days with at least six consecutive days when TX > 90th percentile	days
	ID15	ID15	Annual count when TX (daily maximum) < 15°C	days
	TR20	Tropical nights	Annual count when TN (daily minimum) > 20°C	days

In addition to analysing individual stations, we have analysed trends for the groups of stations in order to investigate their common trend patterns. Five groups were formed based on topographic locations of the stations. We grouped 16 stations from lowlands, 9 stations from valleys, 5 stations from river valleys, 9 stations from the mountain slopes, and 7 stations from the mountain ridges featuring average elevations of 150, 1,204, 1,720, 1,676, and 1,614 m asl, respectively. Here, valleys imply mostly flat and wide valleys, whereas river valleys imply mostly v-shaped deep valleys. The trend magnitude of a particular group is estimated as the average trend of all stations participating in that group. To further show the inter-annual variability of temperature indices, anomalies of individual stations calculated against the period of 1981–2010 were averaged over whole Nepal.

3.2.3 | Investigation of circulation and cloud cover change

We examined the influence of circulations characteristics, cloud cover, and moisture variables on mean and extreme temperature trends based on the ERA-Interim reanalysis (Dee *et al.*, 2011), which captures the seasonal and spatial variations of temperature trends over Nepal (Supporting Information Figure S1). For the quantitative comparison with temperatures, trends of the ERA-Interim cloud cover were also assessed for the grid cells collocating station locations.

4 | RESULTS

4.1 | Trends in mean seasonal temperatures

4.1.1 | Mean seasonal maximum temperature

Trend estimates and their significance for the mean seasonal T_{max} time series of all stations are presented in Figure 2. In general,

Figure 2 suggests significant and widespread warming trends in all the seasons, although the magnitude and significance vary across seasons. More than 90% of the stations feature warming trends for monsoon and pre-monsoon seasons (Figure 3), where such trends are significant for around two-third of the total stations. Conversely, percentages of stations with warming trends are lower in winter (64%) and post-monsoon (82%), where such warming is significant only at 45% of the total stations. The low number of stations with significant warming trends in winter and post-monsoon is mainly due to the significant cooling trends in the southern lowlands. Overall, pre-monsoon is characterized by the highest rate of warming (~0.05°C·year^{-1}). Mean trends for the rest of seasons account to ~0.025–0.036°C·year^{-1}, where the annual average warming is around 0.04°C·year^{-1}.

Magnitude of warming in T_{max} is highest at the mountain ridges (0.07°C·year^{-1}) and slopes (0.05°C·year^{-1}) and the lowest in lowlands (0.01°C·year^{-1}) and river valleys (0.02°C·year^{-1}) through the year (Figure 4). These findings indicate that the magnitude of warming is influenced by terrain features rather than by elevation differences. For instance, stations mostly concentrated within the mountain valleys do not experience increased warming with elevation—termed as the elevation-dependent warming (EDW)—for all the seasons, except for winter (Figure 5). The distinct EDW during winter can be explained by cooling trend in lowlands (0.02°C·year^{-1}) but warming trend in mountain regions (0.08°C·year^{-1}). There is a weak EDW during monsoon, possibly due to a widespread influence of moisture, cloudiness and precipitation on temperatures. In general, lowlands feature lower warming trends (<0.02°C·year^{-1}) than the mountain regions (>0.03°C·year^{-1}) in all seasons.

4.1.2 | Mean seasonal minimum temperature

Although general warming is evident in mean seasonal T_{min} as well, however, their magnitude and significance are
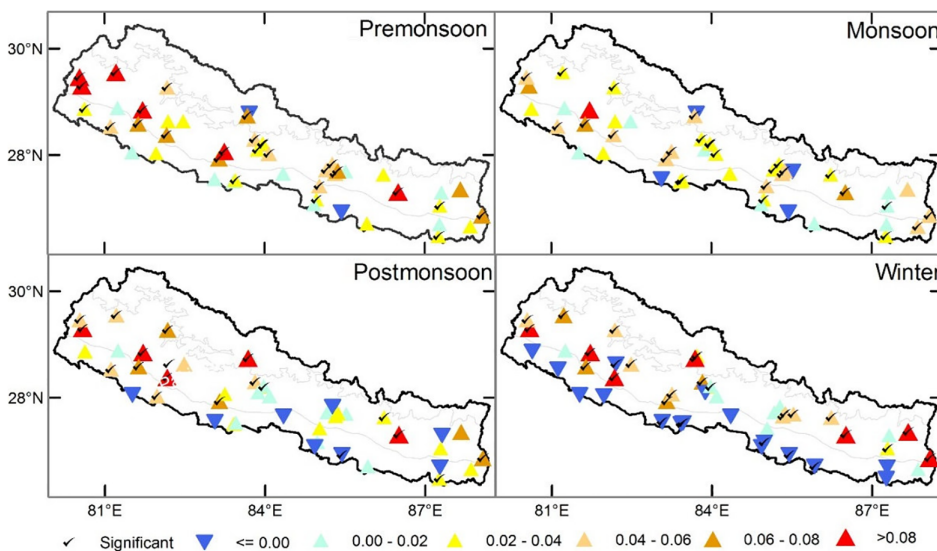

FIGURE 2 Station wise trend (°C·year^{-1}) for seasonal T_{max} temperature. Three broad physiographic regions (south to north), are shown. Ticks indicate statistical significance of trends [Colour figure can be viewed at wileyonlinelibrary.com]

FIGURE 3 Percentage of total number of stations featuring different trend characteristics for temperature extreme indices [Colour figure can be viewed at wileyonlinelibrary.com]
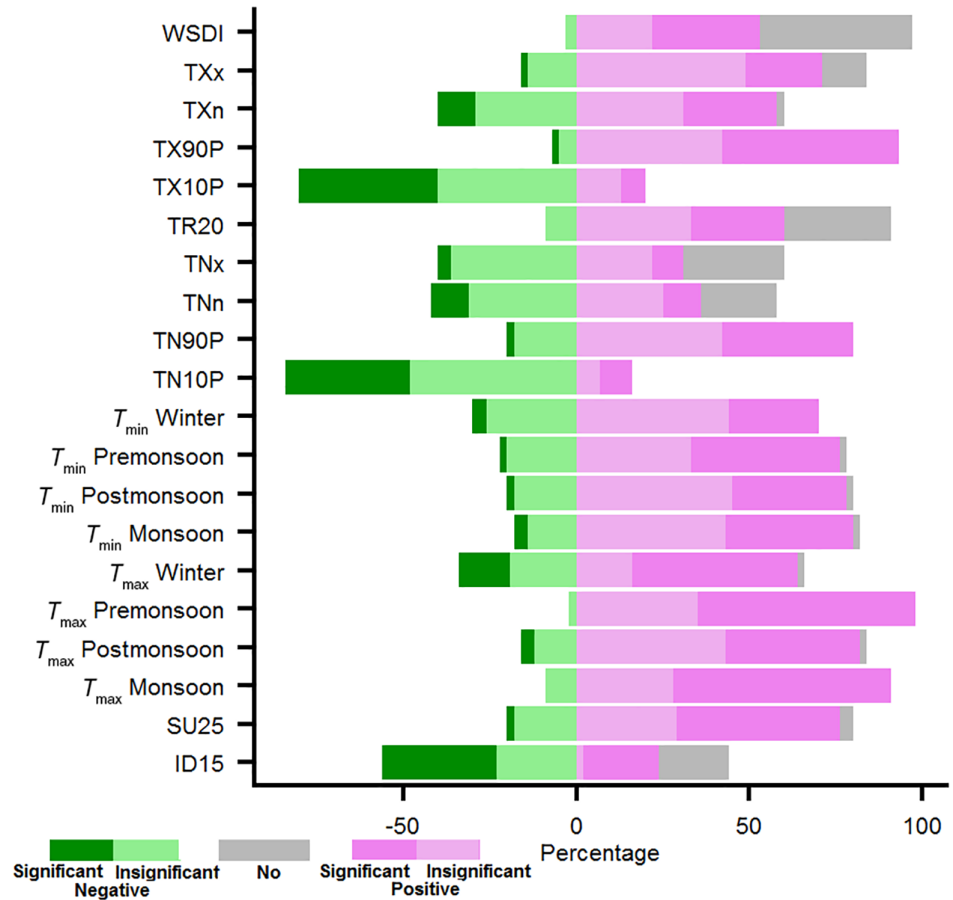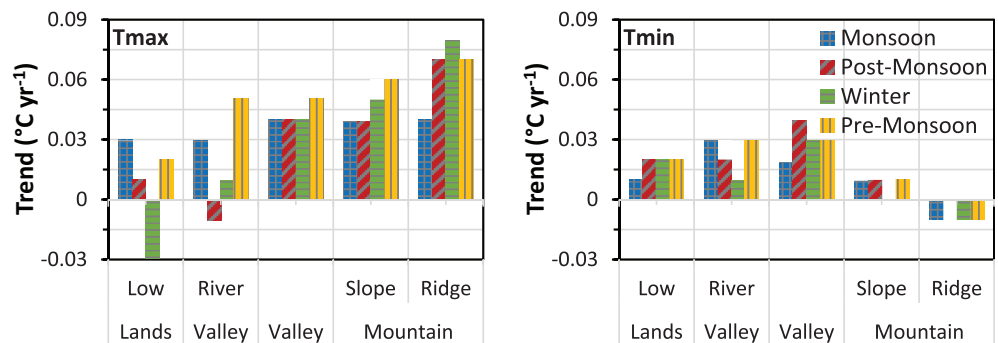

FIGURE 4 Mean seasonal maximum (T_{max}) and minimum (T_{min}) temperature trends in different topographic features [Colour figure can be viewed at wileyonlinelibrary.com]

relatively weaker compared with that of T_{max} (Figure 6). Additionally, inter-seasonal variation of warming trends is relatively low. Overall, only 70–80% of all stations show warming trends and only 26–43% of those trends are found statistically significant (Figure 3).

Consistent with T_{max} warming, a majority of stations features significant warming in T_{min} during pre-monsoon and monsoon seasons, whereas the highest warming is observed during pre-monsoon and post-monsoon seasons. Magnitude of warming is mostly below 0.04°C·year^{-1} throughout the year with an annual average of 0.02°C·year^{-1}. Significant cooling observed over lowlands in T_{max} is weaker in T_{min}. Furthermore, mountain ridges feature slight cooling in T_{min}

in contrast to strong warming in T_{max}, throughout the year. There is no clear elevation dependence of T_{min} in any of the seasons (Figure 5).

The magnitude of trend in mean temperature (0.03°C·year^{-1}) calculated from the mean temperature time series ($T_{mean} = [T_{max}+T_{min}]/2$) is similar to the statistical average of trends in T_{max} (0.04°C·year^{-1}) and T_{min} (0.02°C·year^{-1}). Overall, T_{mean} trend pattern is dominated by trends in T_{max} (Figure 7). Consistent with T_{max}, more than 90% stations feature warming in T_{mean}, which is significant at two third of the stations, particularly for pre-monsoon and monsoon seasons. In summary, warming in the region mainly attributes to warming in T_{max}.
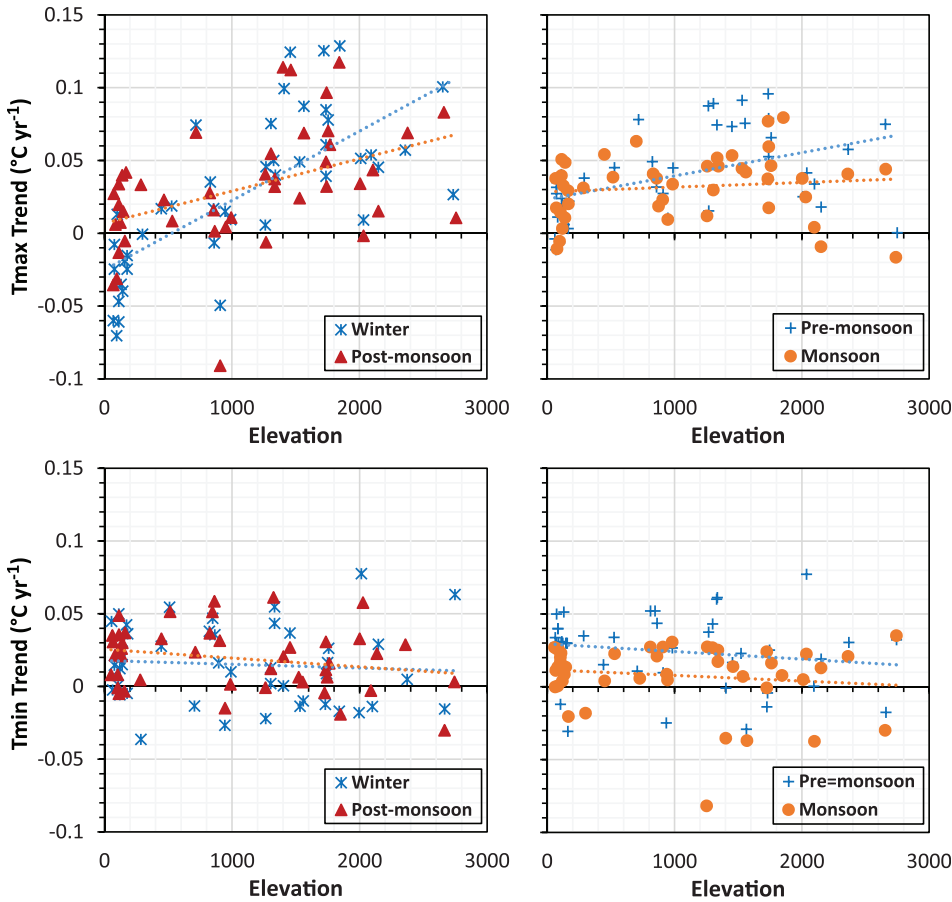
FIGURE 5 Elevational dependence of warming of T_{max} and T_{min} in different seasons [Colour figure can be viewed at wileyonlinelibrary.com]
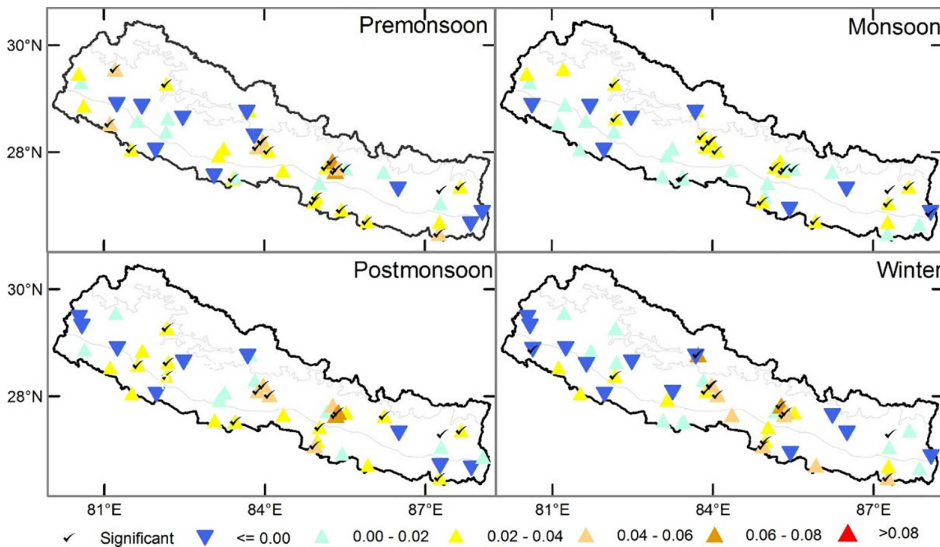

FIGURE 6 Same as Figure 2 but for mean seasonal T_{min} trend (°C·year^{-1}) [Colour figure can be viewed at wileyonlinelibrary.com]

4.2 | Trends in extreme temperature indices

4.2.1 | Absolute indices

Annual trends of absolute extreme temperature indices (maximum and minimum of T_{max}, as well as of T_{min}) are shown in Figure 8. T_{max} extreme indices suggest warming at a majority of stations, whereas T_{min} indices show a mixed pattern. Around 70% of all stations feature increase in TXx,

which is significant at 22% of the stations, mostly concentrated in mountain regions. An average increase in TXx is estimated to 0.03°C·year^{-1} (Figures 3 and 8). In contrast to TXx, TXn features contrasting patterns for mountains and lowlands, suggesting significant warming for the most of stations from mountain regions but cooling for all the stations from lowlands (Figure 9). The mean rate of warming is 0.03°C·year^{-1}. TNx and TNn have mixed trends and about

FIGURE 7 Same as Figure 2 but
for mean seasonal temperature (T_{mean})
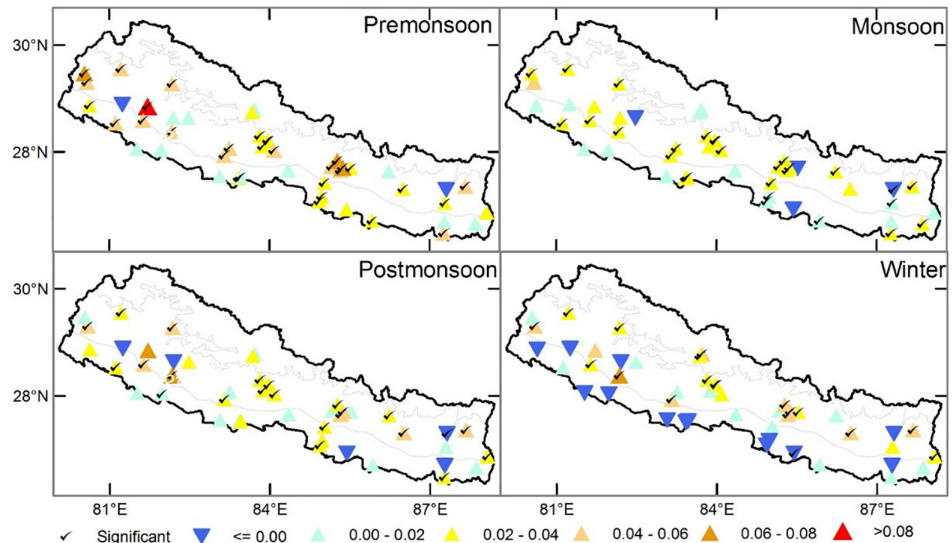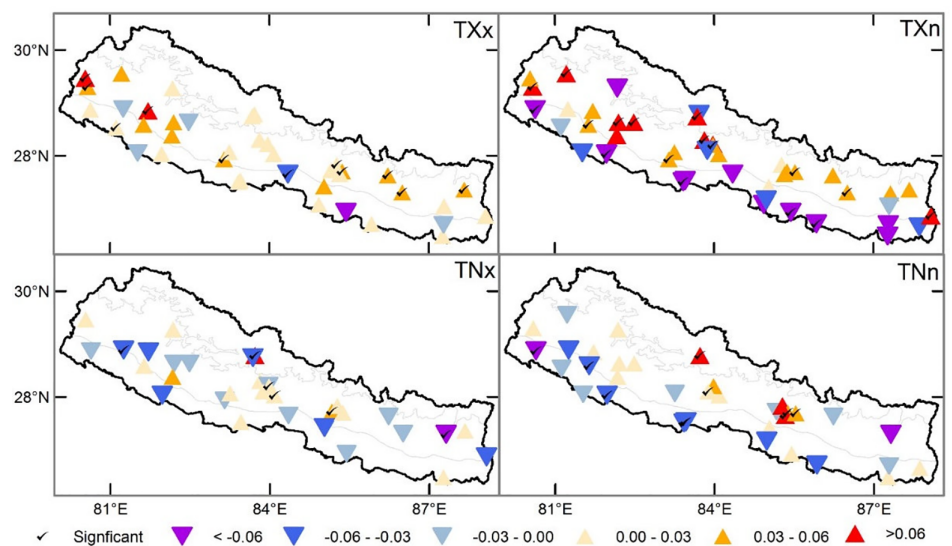trends (°C·year^{-1}) [Colour figure can
be viewed at wileyonlinelibrary.com]

FIGURE 8 Same as Figure 2 but
for annual absolute extreme
temperature indices trends (°C·year^{-1})
[Colour figure can be viewed at
wileyonlinelibrary.com]

25% of the stations feature no trend. Average increase across the country for both indices is lower than 0.01°C·year^{-1}.

4.2.2 | Percentile-based indices

Our results show statistically significant rising trends for warm temperature indices (warm nights and days; TN90P and TX90P) and significant negative trends for cool temperature indices (cool nights and days; TN10P and TX10P). However, changes in magnitude and significance are not uniform for all four indices. Rise in the number of warm days is considerably pronounced, featuring a positive trend at 93% and a significant positive trend at 51% of all stations, accounting to a mean decadal increase of 13 days. Warm nights show an increase at 80% of the stations and a significant increase at 38% of the stations, amounting to a mean decadal increase of 4 days (Figures 3 and 10). These findings indicate higher warming during daytime than during nighttime. Conversely, cool days (TX10P) and cool nights (TN10P) exhibit negative trends at about 80% of all stations and significant negative trends at about 38% of all stations, amounting to a mean decadal decrease of 6 days. Overall, percentile-based indices show clear patterns of extreme temperature trends compared with other indices. Significant warming across the country is evident, which is consistent with warming in the mean seasonal maximum temperatures.

The analysis of trends at stations with different terrain characteristics reveals that T_{max}-based indices are particularly influenced by the surrounding terrain. A clear gradient of trends from mountain slopes and ridges to the lowlands and valleys is apparent in the results. In contrast, no such pattern is observed for T_{min}-based indices. For instance, increasing (decreasing) trend of warm days (cold days) intensifies from lowlands and valleys to mountain slopes and ridges (Figure 9). Noticeably, few stations concentrated in lowlands exhibit an increase in cool days, which contrasts to an overall
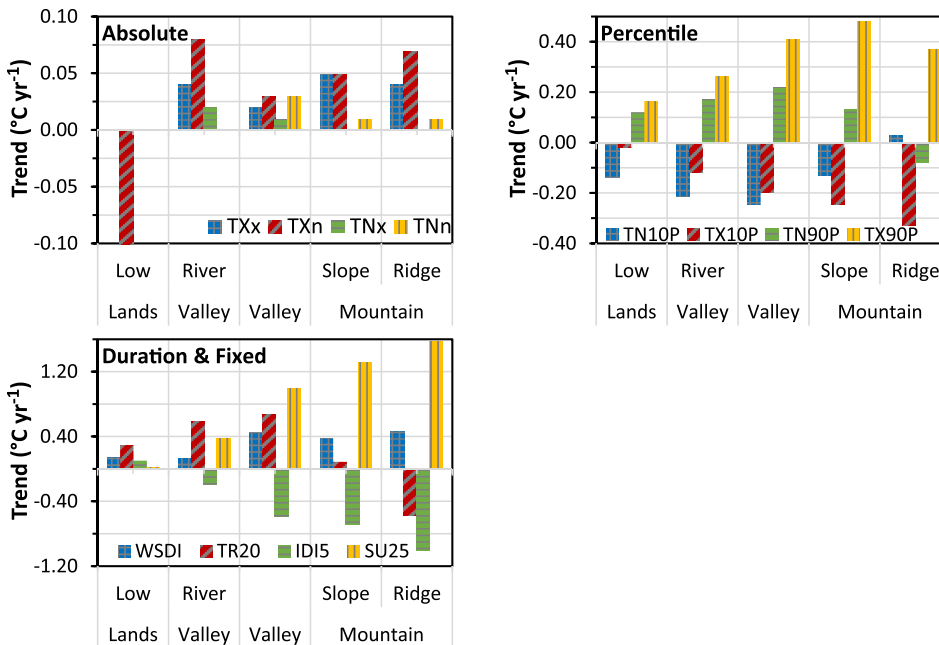
FIGURE 9   Trends of annual extreme temperature indices in different topographic features [Colour figure can be viewed at wileyonlinelibrary.com]
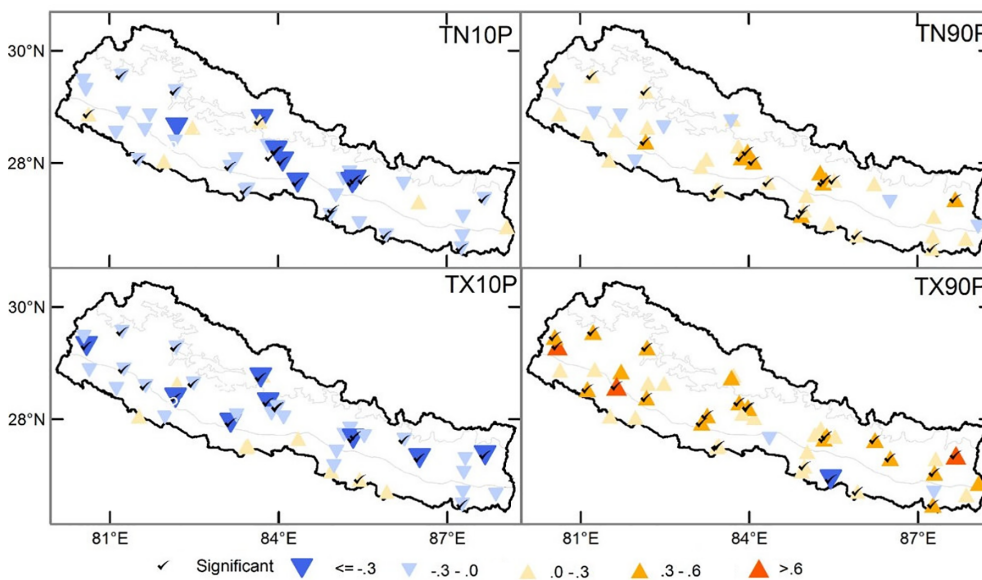

FIGURE 10   Same as Figure 2 but for trends of percentile-based annual extreme temperature indices (%·year^{-1}) [Colour figure can be viewed at wileyonlinelibrary.com]

warming pattern. Apparently, T_{min}-based indices feature opposite trend patterns compared with T_{max}-based indices for different terrain features (Figure 9). Mountain ridges experience cooling in T_{min}-based indices (i.e., a decrease in warm nights and increase in cold nights).

4.2.3 | Duration- and threshold-based indices

Annual number of days with T_{max} less than 15°C (ID15) features contrasting pattern for mountains and lowlands (Figure 11). ID15 has increased at all the stations from lowlands and decreased at almost all the stations from mountain regions. ID15 representation is equivalent to cool days in the

lowlands. Thus, the patterns are consistent and support the cooling tendency at low elevations.

The number of summer days (SU25) shows a positive trend at the most of the stations (76%) with higher magnitude and significance of warming in mountain regions than in lowlands. Significant positive trends are found at 47% of all stations. The mean increase in SU25 is estimated to be around 9 days per decade (Figure 11). Although the majority of stations suggest an increase in tropical nights (TR20) and warm spell duration (WSDI), about 40% of all stations are trendless. Considering different terrain features, the positive trend of summer days, and warm spell duration are broadly similar to that of warm day index. The strongest trend of warming days is observed in mountain regions (Figure 9).

FIGURE 11 Same as the
Figure 2 but for trends of duration- and
threshold-based annual extreme
temperature indices (days·year^{-1})
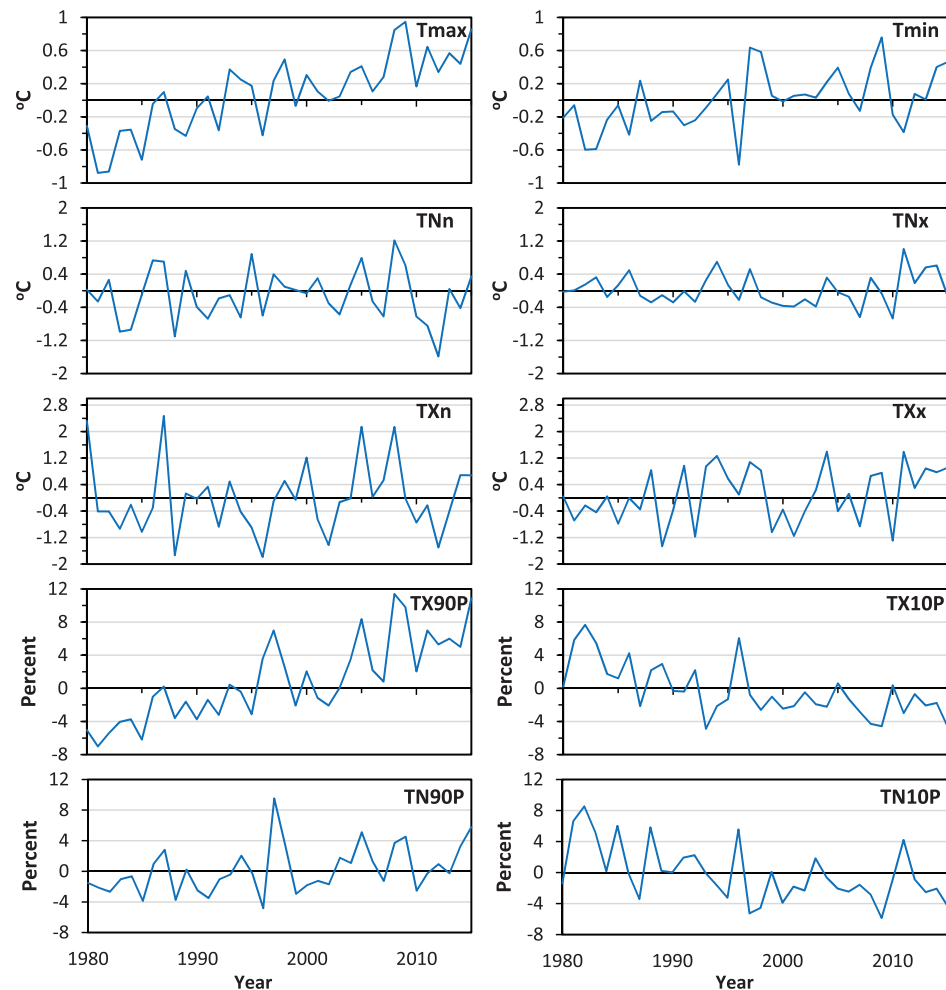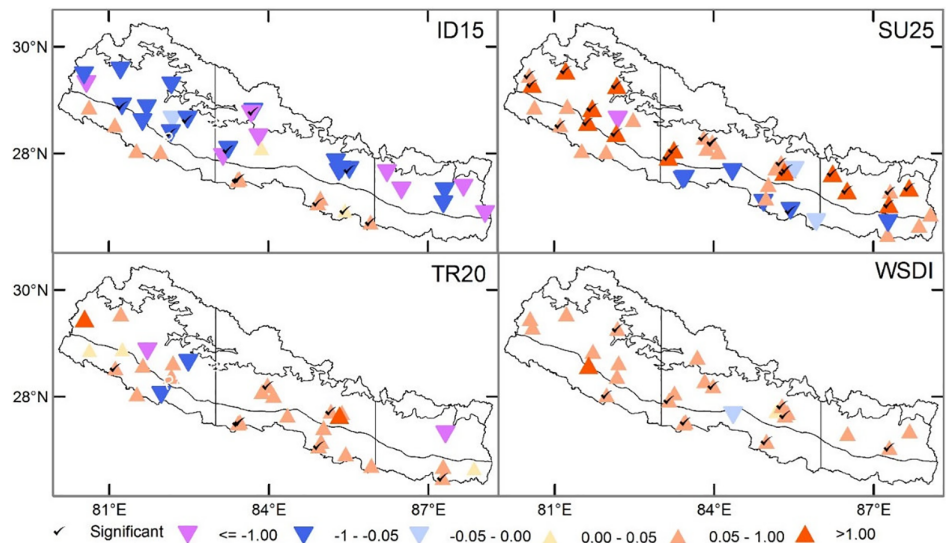[Colour figure can be viewed at
wileyonlinelibrary.com]

FIGURE 12 Time series of inter-
annual country average anomalies for
different annual temperature indices for
the period of 1980–2016 relative to the
1981–2000 normal period [Colour
figure can be viewed at
wileyonlinelibrary.com]

Summarizing, the country-averaged time series reflects the temperature trends from individual stations for all the indices (Figures 12 and 13), although stations in different subregions show a slightly deviant behaviour. Trends from a majority of stations are positive, except for T_{max} over lowlands during winter and post-monsoon. In general, T_{max}-based indices show more pronounced warming and a positive trend of warm extreme events, whereas for cool extremes, negative trends are apparent across Nepal. In particular, positive anomalies are noted for mean annual T_{max}, summer days, and warm
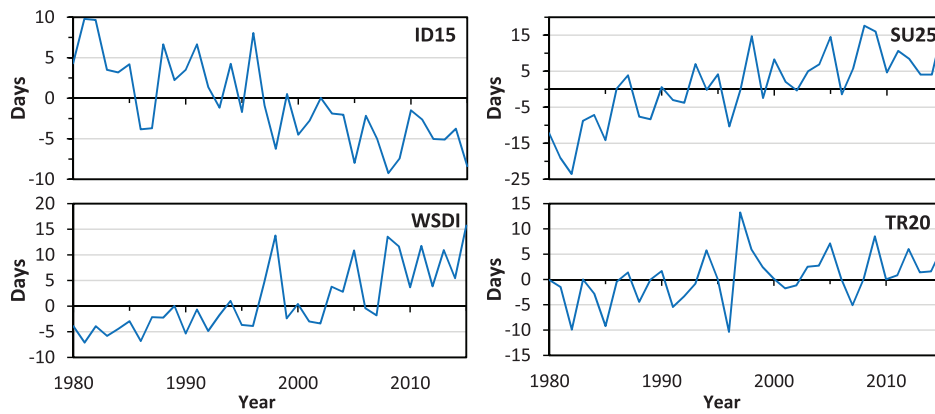
FIGURE 13 Same as the Figure 12 but for ID15, SU25, WSDI, and TR20 temperature indices [Colour figure can be viewed at wileyonlinelibrary.com]
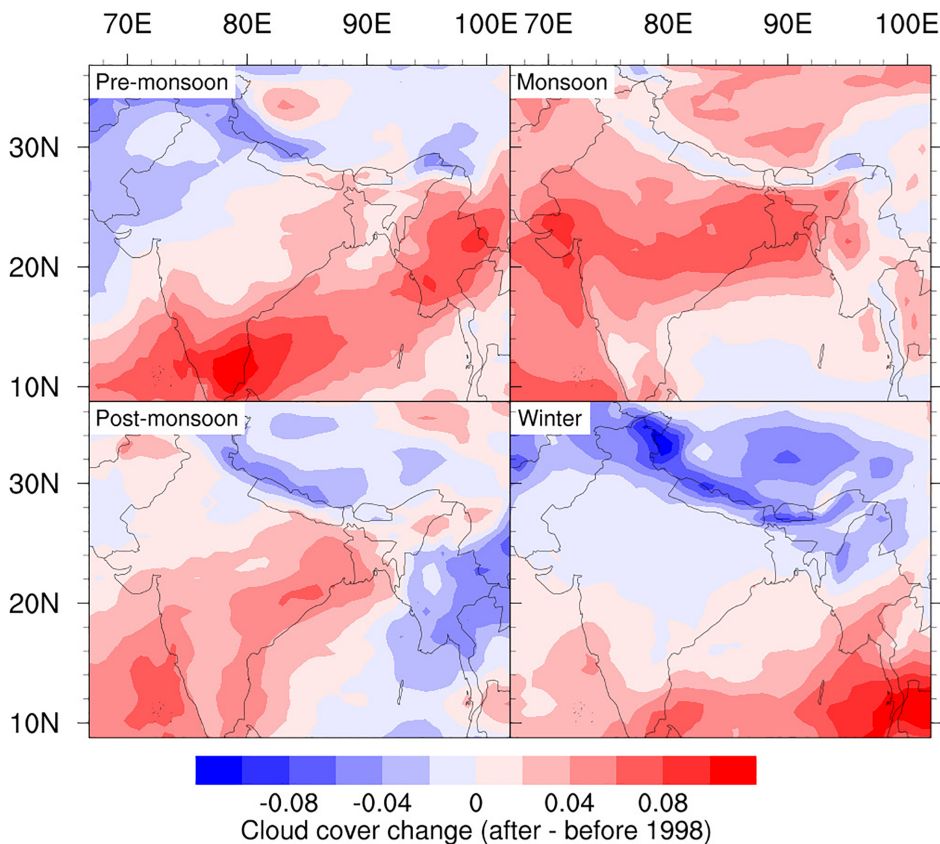

FIGURE 14 Difference in pre-1997 and post-1997 seasonal cloud cover from the ERA-Interim reanalysis [Colour figure can be viewed at wileyonlinelibrary.com]

days for all the years after 1997. The year 2010 was the hottest year of the analysis period. Furthermore, negative anomalies for cool days are observed, which indicate an accelerated warming after 1997.

4.3 | Influence of changing circulation and cloud cover

Besides an increase in the net radiations due to anthropogenic greenhouse gas emissions, change in circulation features and variation in cloud cover can potentially explain changes in temperature and precipitation in different regions. For instance, the far

above global average warming in Nepal and cooling in southern lowlands are likely influenced by changing circulation characteristics at large to local scale as well as by climate change feedbacks.

Figure 14 shows that cloud cover over Nepal derived from the ERA-Interim reanalysis is declining after the year 1997 in all seasons except monsoon, which is likely caused by anticyclonic anomalies in the mid-to-upper troposphere over the central Himalayan region in recent decades (Figure 15). Although cloud reduction during monsoon is relatively small but it is uniform across the entire region. This partly explains the uniform rate of warming in Nepal during monsoon, however, attribution of temperature increase to changes in cloud cover is not yet

FIGURE 15 Pre-1997 and Post-1997 differences in historical winds (vector) and geopotential heights (shaded) for difference seasons and pressure levels from the ERA-Interim reanalysis [Colour figure can be viewed at wileyonlinelibrary.com]
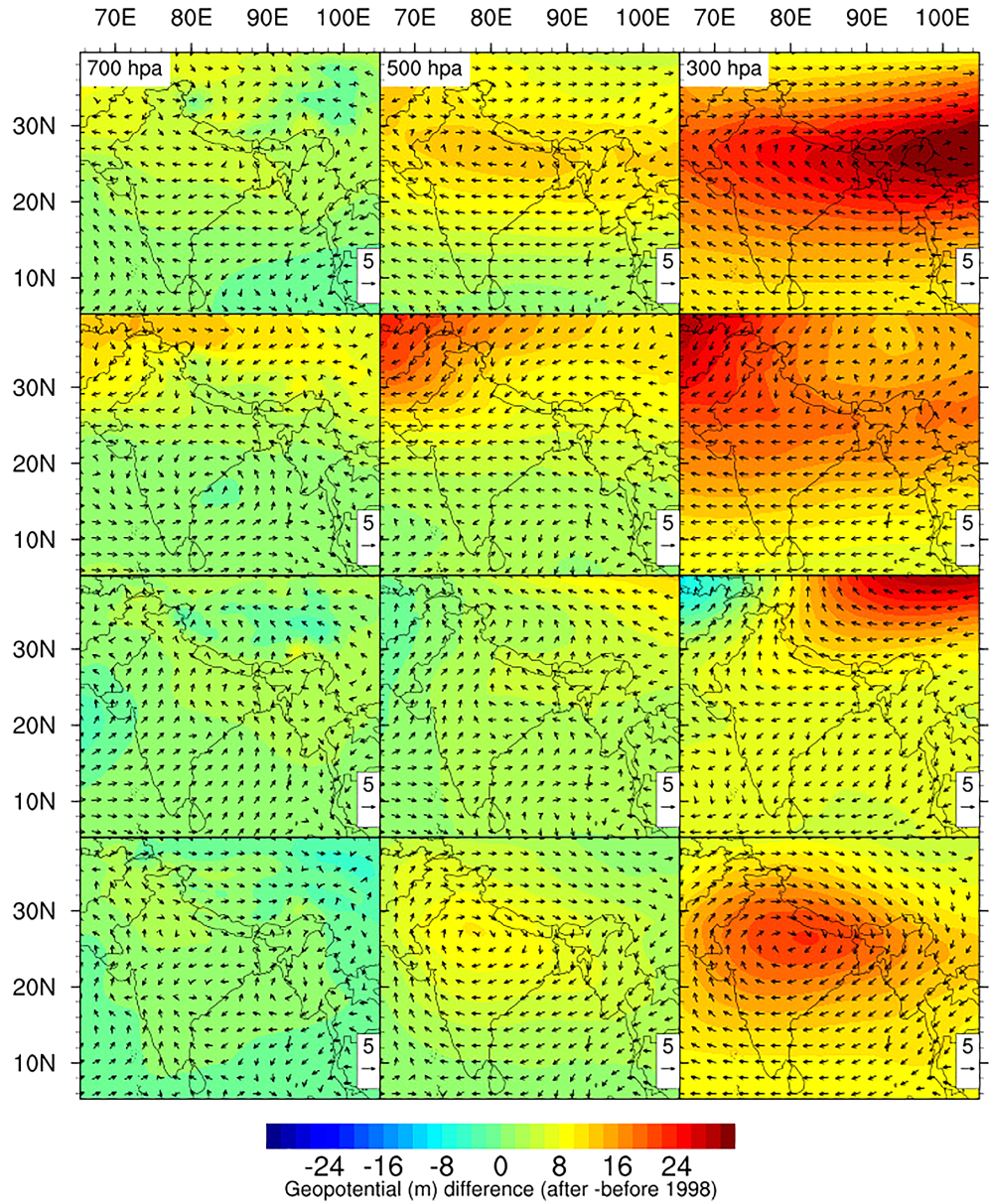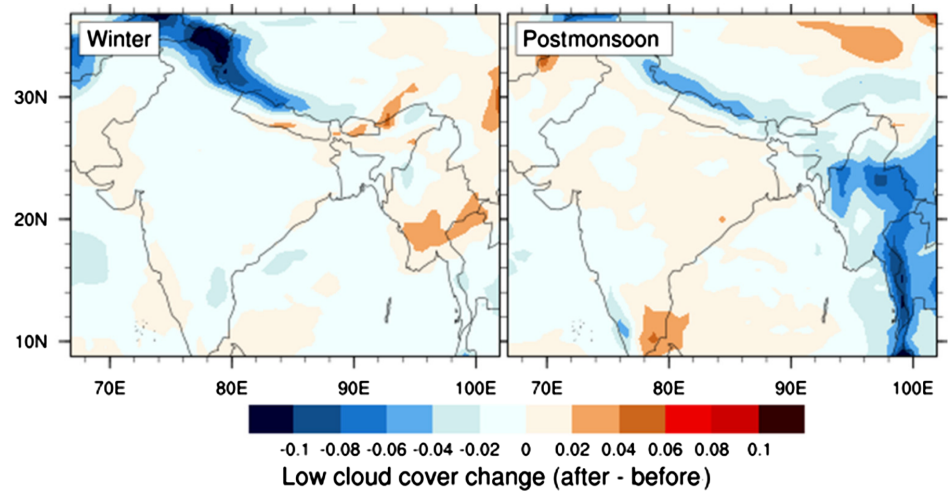

FIGURE 16 Pre-1997 and post-1997 differences in the seasonal low cloud cover from the ERA-Interim reanalysis [Colour figure can be viewed at wileyonlinelibrary.com]
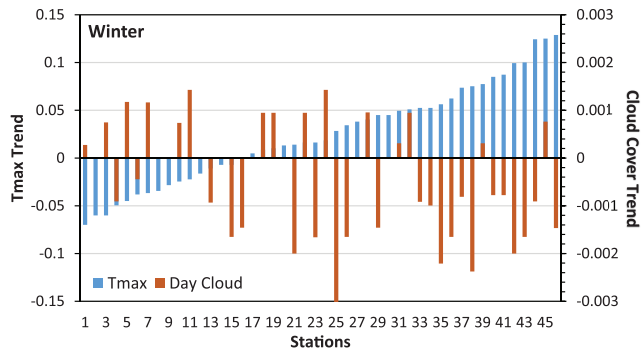
FIGURE 17 Linear trends of T_{max} (°C·year^{-1}) from observations and day time cloud cover (fraction Year^{-1}) at station locations (derived from ERA-Interim) for winter [Colour figure can be viewed at wileyonlinelibrary.com]

confirmed. Similarly, a significant decrease in cloud cover observed over mountainous regions is consistent with a significant increase in T_{max} there, whereas increase in cloud cover over parts of lowlands is consistent with cooling observed there, during non-monsoon months. Contrasting trends patterns for mountain and lowland regions during winter for T_{max} is verifiable from comparison of T_{max} and daytime cloud cover trends at station locations as well, where increase (decrease) in cloud cover is largely consistent with a decrease (increase) in T_{max} (Figure 16). However, station level relation is relatively low for other seasons, probably due to coarse resolution of the ERA-Interim cloud cover (not shown).

Furthermore, increase in low-level cloud cover over lowlands explains increase in fog episodes in recent decades (Figure 17) and associated T_{max} cooling during winter. A number of recent studies have confirmed increasing frequency and prolongation of fog episodes over the Indo-Gangetic plains and over the adjacent lowlands of Nepal, particularly after 1997 (Syed *et al.*, 2012; Shrestha *et al.*, 2017; Hingmire *et al.*, 2018; Shrestha *et al.*, 2018). Conducive environment for such phenomenon is provided by upper tropospheric (above 700 hPa) high-pressure anomalies evident during winter and post-monsoon after 1997 over the region (Figure 15), which favours increase in the boundary layer stability (Syed *et al.*, 2012; Hingmire *et al.*, 2018). However, land use and land cover change as well as increase in atmospheric aerosols in the region might also influence the fog formation over the southern Nepal.

5 | DISCUSSIONS

5.1 | Other possible mechanisms influencing temperature trends

Besides large-scale atmospheric processes, temperature distribution in complex mountainous terrain is highly influenced

by topographic features, such as, slope, aspect, and curvature, by surface characteristics, namely, land cover, land use, land management, and local winds (Mahrt, 2006; Minder *et al.*, 2010; Kattel *et al.*, 2013; Gerlitz *et al.*, 2016). For instance, present study finds the highest warming at mountain slopes and ridges, particularly for T_{max}. This is because the fact that surface features of snow and glacier strongly control the temperature distribution and its changes at high altitudes via the snow-albedo effect. A decreased snowfall and reduction of snow cover due to a warmer climate lead to a reduced snow albedo, and subsequently, higher absorption of solar radiation at the surface, resulting in enhanced warming in mountain regions (Pepin *et al.*, 2015; Minder *et al.*, 2018). Such snow albedo-effect has already been identified as a dominant driver for amplification of warming at high elevations and in the Himalayas (Pepin *et al.*, 2015; Palazzi *et al.*, 2018). Observed EDW for T_{max} during winter can also be related to significant influence of the snow-albedo effect. The fact that EDW has not been detected for T_{min} further supports this finding (Figure 5). It is pertinent to mention that the effect of changing snow cover on observed warming could only be explored for winter as the stations considered here are mainly located below 3,000 m asl and the snow line in Nepal descends below this height usually during winter only (Lang and Barros, 2004; Norris *et al.*, 2016). Most likely, the inclusion of high elevation stations can provide further insight into EDW for warm seasons. Conversely, a reduction in summer and winter snow cover detected in recent decades in the Himalayas is likely a result of anticyclonic anomalies in the upper troposphere and associated regional warming (Norris *et al.*, 2018).

Land use and land cover changes influence the temperature change due to their influence on sensible and latent heat partitioning of the available energy. For instance, barren and dry surfaces favour the sensible heat release (warming), whereas moist and forest or snow covered surfaces favour the latent heat release and trigger local cooling. Thus, urbanization and deforestation may have contributed to enhanced warming in Nepal (Kattel and Yao, 2013; Nayava *et al.*, 2017). Confirming this, however, requires a comprehensive assessment, which is beyond the scope of present study.

5.2 | Consistency with other studies and observed impacts in different sectors

Our results are generally consistent with the findings of previous local to regional level studies but with some noticeable differences in terms of trend magnitudes and their distribution (e.g., Shrestha *et al.*, 1999, 2017; Sharma *et al.*, 2000; Baidya *et al.*, 2008; Caesar *et al.*, 2011; Kattel and Yao, 2013; Sheikh *et al.*, 2015; Nepal, 2016; Nayava *et al.*,

2017). Overall, the results suggest an increased mean seasonal warming, rising warm extremes, and declining cold extremes across the country, except for the southern lowlands. There is a clearer, consistent and stronger warming in T_{max}-based seasonal means and annual extreme indices than for T_{min}, indicating higher rate of warming during the day than during the night. This typical diurnal warming pattern over the Himalaya seems to be a unique feature, which has been previously reported by Baidya et al. (2008) and Shrestha et al. (1999). In contrast, prominent warming of T_{min}-based indices has been reported for the Tibetan plateau, inner Mongolia, indo-pacific regions, and whole globe (Alexander et al., 2006; Caesar et al., 2011; Donat et al., 2013; Shrestha et al., 2017; Ding et al., 2018; Tong et al., 2019). Furthermore, we noted that the magnitude of T_{max} warming ($0.04°C \cdot year^{-1}$) detected over the 1980–2016 period in the present study is slightly lower than $0.06°C \cdot year^{-1}$ as reported by Shrestha et al. (1999) for the 1971–1994 period across Nepal. Furthermore, we observed the highest rates of warming during pre-monsoon, whereas Shrestha et al. (1999) have reported highest warming during post-monsoon seasons. Such contrast between the two studies may possibly arise due to differences in their periods of analyses, employed trend detection methods and extensive quality control applied by the present study. Nevertheless, higher daytime warming over mountain regions persists in time. Significant warming of T_{max} seasonal and annual means and extremes and increase in the number of summer days, number of warm days (cool days), and duration of warm spell indicate an accelerated warming after 1997, as suggested by Kattel and Yao (2013).

We provided an overview of possible factors influencing the mean and extreme temperature trends, however, the quantification of relative contribution from different factors requires further investigation. Nevertheless, the impacts of observed warming on different climate sensitive environments as well as on the Nepali economy is already well acknowledged. Thinning and retreat of glaciers, reduced snow cover, enhanced formation and expansion of glacial lakes, upward shift of treeline ecotone and consequential migration of plant and animal species to higher elevations have already been observed. Furthermore, shifting agro-ecological zones, spread of vector borne diseases to non-endemic areas, and increasing frequency and magnitude of hydrometeorological disasters are among the major climate change impacts in the country (Shrestha et al., 1999; Shrestha and Aryal, 2011; Dhimal et al., 2014; Gerlitz, 2014; Dhimal et al., 2015; Aryal et al., 2016; Schickhoff et al., 2016; Soncini et al., 2016; Karki et al., 2017a; Talchabhadel et al., 2018).

Although the overall increase in temperature is comparably low in the lowlands, prolonged periods of fog-related cold waves during winter have become one of the major threats for the population of the warmest part of the country. On average, 72 people died annually between 2003 and 2013 due to cold waves (DesInventar, 2018). Lowlands are also highly exposed to heat wave disasters as temperature in pre-monsoon and early monsoon frequently exceeds 40°C. The pronounced increase in mean temperature, warm spell duration, summer days, tropical nights, and hot days and nights involve an increasing risk for human activities in mountain regions, where poor infrastructure impedes to cope with the heat. Particularly, an increase in heavy precipitation (Karki et al., 2017a) and temperature aggravated the risk of diarrheal diseases, dengue fever, and malaria (Hijioka et al., 2014; Dhimal et al., 2015).

Likewise, increasing mean and extreme temperatures affect the agriculture sector (crop failures due to droughts), water resources (high evaporation and drying), and ecosystem services. The observed changes in precipitation distribution, frequent droughts, and flood episodes in recent decades (Bohlinger and Sorteberg, 2017; Karki et al., 2017a; Talchabhadel et al., 2018) are likely related to observed warming as specific humidity increases with rising temperature. These significant changes in mean and extreme temperatures as well as high exposure and poorly developed adaption strategies makes Nepal and its mountain communities highly vulnerable to climate change impacts (Mainali and Pricope, 2017).

It is pertinent to mention that our study uses only 46 high-quality stations, which poorly represent the spatial completeness over Nepal. High-elevation stations with continuous and high-quality long-term climate data are almost non-existent in Nepal, leading to an analysis gap in the vulnerable high mountain region. A recent addition to the DHM network of automatic weather stations at high elevations (e.g., EVK2CNR in the Khumbu regions and TREELINE project stations in Rolwaling) is invaluable but still insufficient. Conversely, devising adaption strategies for different climate and disaster sensitive sectors for the upcoming century requires historical as well as future changes at high spatial and temporal resolutions. To achieve this objective, historical and future climatic changes can be assessed from the output of robust climate models that have been shown to reasonably reproduce the prevailing climatic characteristics of the region. In this regard, present study can serve as a baseline (Gerlitz et al., 2015; Hasson et al., 2016; Norris et al., 2016; Karki et al., 2017b; Hasson et al., 2018). The climate model simulations can further support in better understanding of the physical processes and mechanisms affecting the spatiotemporal distribution of mean and extreme temperatures, and can particularly be useful for providing future climate change scenarios (Norris et al., 2015, 2018; Karki et al., 2018; Palazzi et al., 2018).

6 | CONCLUSIONS AND SUMMARY

This study presents the spatiotemporal variations of mean seasonal temperatures and extreme temperature indices for the period of 1980–2016 across Nepal, using high-quality continuous data from 46 long-term climatic stations located in different topoclimatic environments. By including a large number of stations and data for recent years, this study provides a detailed and spatially coherent representation of the changes in mean and extreme temperatures for Nepal, and thus, complement the findings of previous studies. Further, possible mechanisms that explain the enhanced warming and the spatially heterogeneous trend patterns over Nepal are discussed. In this context, both, large-scale atmospheric and local-scale terrain and land surface features are considered as potential drivers of observed changes in mean and extreme temperatures.

Our results show a widespread and significant warming across the country, except for winter cooling over the southern lowlands. Warming is observed higher for mean annual T_{max} (~0.04°C·year^{-1}) than for mean annual T_{min} (~0.02°C·year^{-1}), where T_{mean} trend change is around 0.03°C·year^{-1}. Similarly, significant rising trend is observed for temperature extremes across Nepal, which is stronger for T_{max}-based indices than for T_{min}-based indices. Warm extremes are increasing and cold extremes are decreasing across the country. Accelerated trend for T_{max}-based indices after 1997 points towards a climate regime shift. We show that the rate of warming is sensitive to different topographic and physiographic regions, as higher warming in T_{max}-based indices is detected at mountain slopes and ridges as compared with higher trend changes detected in T_{min} over lowlands and in river valleys. Generally, warming trends are observed stronger during pre-monsoon season. However, highest winter warming observed for T_{max} over mountain slopes and ridges can be attributed to decreasing snow cover extent and cloud cover owing to strengthening of anticyclonic circulation in the mid-to-upper troposphere during non-monsoon seasons and a weakening of near-surface flow during monsoon season in recent decade. Furthermore, a slight winter cooling observed over the southern lowlands is likely triggered by prolonged and more frequent fog episodes and increased cloud cover due to increased atmospheric stability in the lower troposphere in recent decades. These mechanisms explain the observed spatiotemporal variations of mean and extreme temperature trends across Nepal.

ORCID

Ramchandra Karki https://orcid.org/0000-0002-3742-1015
Shabeh ul Hasson https://orcid.org/0000-0002-7791-9635
Rocky Talchabhadel https://orcid.org/0000-0003-0526-7663
Jürgen Böhner https://orcid.org/0000-0002-0842-0152

REFERENCES

Alexander, L.V., Zhang, X., Peterson, T.C., Caesar, J., Gleason, B., Klein Tank, A.M.G., Haylock, M., Collins, D., Trewin, B., Rahimzadeh, F., Tagipour, A., Rupa Kumar, K., Revadekar, J., Griffiths, G., Vincent, L., Stephenson, D.B., Burn, J., Aguilar, E., Brunet, M., Taylor, M., New, M., Zhai, P., Rusticucci, M. and Vazquez-Aguirre, J.L. (2006) Global observed changes in daily climate extremes of temperature and precipitation. *Journal of Geophysical Research Atmospheres*, 111(5), 1–22. https://doi.org/10.1029/2005JD006290.

Aryal, A., Shrestha, U.B., Ji, W., Ale, S.B., Shrestha, S., Ingty, T., Maraseni, T., Cockfield, G. and Raubenheimer, D. (2016) Predicting the distributions of predator (snow leopard) and prey (blue sheep) under climate change in the Himalaya. *Ecology and Evolution*, 6, 4065–4075. https://doi.org/10.1002/ece3.2196

Baidya, S.K., Shrestha, M.L. and Sheikh, M.M. (2008) Trends in daily climatic extremes of temperature and precipitation in Nepal. *Journal of Hydrology and Meteorology*, 5(1), 47–50.

Bhutiyani, M.R., Kale, V.S. and Pawar, N.J. (2007) Long-term trends in maximum, minimum and mean annual air temperatures across the Northwestern Himalaya during the twentieth century. *Climatic Change*, 85, 159–177. https://doi.org/10.1007/s10584-006-9196-1.

Bohlinger, P. and Sorteberg, A. (2017) A comprehensive view on trends in extreme precipitation in Nepal and their spatial distribution. *International Journal of Climatology*, 38, 1833–1845. https://doi.org/10.1002/joc.5299.

Böhner, J. and Lehmkuhl, F. (2006) Environmental change modelling for central and high Asia: Pleistocene, present and future scenarios. *Boreas*, 34(2), 220–231. https://doi.org/10.1111/j.1502-3885.2005.tb01017.x.

Böhner, J., Miehe, G., Miehe, S. and Nagy, L. (2015) Climate and weather variability: an introduction to the natural history, ecology, and human environment of the Himalayas, a companion volume to

the flora of Nepal. *Royal Botanic Garden Edinburgh*, 2015(4), 23–89.

Caesar, J., Alexander, L.V., Trewin, B., Tse-ring, K., Sorany, L., Vuniyayawa, V., Keosavang, N., Shimana, A., Htay, M.M., Karmacharya, J., Jayasinghearachchi, D.A., Sakkamart, J., Soares, E., Hung, L.T., Thuong, L.T., Hue, C.T., Dung, N.T.T., Hung, P.V., Cuong, H.D., Cuong, N.M. and Sirabaha, S. (2011) Changes in temperature and precipitation extremes over the Indo-Pacific region from 1971 to 2005. *International Journal of Climatology*, 31(6), 791–801. https://doi.org/10.1002/joc.2118.

Dee DP, Uppala SM, Simmons AJ, Berrisford P, Poli P, Kobayashi S, Andrae U, Balmaseda MA, Balsamo G, Bauer P, Bechtold P, Beljaars ACM, van de Berg L, Bidlot J, Bormann N, Delsol C, Dragani R, Fuentes M, Geer AJ, Haimberger L, Healy SB, Hersbach H, Hólm E V, Isaksen L, Kållberg P, Köhler M, Matricardi M, McNally AP, Monge-Sanz BM, Morcrette J-J, Park B-K, Peubey C, de Rosnay P, Tavolato C, Thépaut J-N, Vitart F. 2011. The ERA-Interim reanalysis: configuration and performance of the data assimilation system. *Quarterly Journal of the Royal Meteorological Society*. 137(656): 553–597. DOI: https://doi.org/10.1002/qj.828.

Dhimal, M., Ahrens, B. and Kuch, U. (2015) Climate change and spatiotemporal distributions of vector-borne diseases in Nepal—a systematic synthesis of literature. *PLoS One*, 10(6), 1–31. https://doi.org/10.1371/journal.pone.0129869.

Dhimal, M., O'Hara, R.B., Karki, R., Thakur, G.D., Kuch, U. and Ahrens, B. (2014) Spatio-temporal distribution of malaria and its association with climatic factors and vector-control interventions in two high-risk districts of Nepal. *Malaria Journal*, 13(1), 457. https://doi.org/10.1186/1475-2875-13-457.

Ding, J., Cuo, L., Zhang, Y. and Zhu, F. (2018) Monthly and annual temperature extremes and their changes on the Tibetan Plateau and its surroundings during 1963–2015. *Scientific Reports*, 8(1), 1–23. https://doi.org/10.1038/s41598-018-30320-0.

Donat, M.G., Alexander, L.V., Yang, H., Durre, I., Vose, R., Dunn, R. J.H., Willett, K.M., Aguilar, E., Brunet, M., Caesar, J., Hewitson, B., Jack, C., Klein Tank, A.M.G., Kruger, A.C., Marengo, J., Peterson, T.C., Renom, M., Oria Rojas, C., Rusticucci, M., Salinger, J., Elrayah, A.S., Sekele, S.S., Srivastava, A.K., Trewin, B., Villarroel, C., Vincent, L.A., Zhai, P., Zhang, X. and Kitching, S. (2013) Updated analyses of temperature and precipitation extreme indices since the beginning of the twentieth century: the HadEX2 dataset. *Journal of Geophysical Research Atmospheres*, 118(5), 2098–2118. https://doi.org/10.1002/jgrd.50150.

Duncan, J.M.A. and Biggs, E.M. (2012) Assessing the accuracy and applied use of satellite-derived precipitation estimates over Nepal. *Applied Geography*, 34, 626–638. https://doi.org/10.1016/j.apgeog.2012.04.001.

Gerlitz, L. (2014) Using fuzzified regression trees for statistical downscaling and regionalization of near surface temperatures in complex terrain: a case study from Khumbu Himal. *Theoretical and Applied Climatology*, 122(1–2), 337–352. https://doi.org/10.1007/s00704-014-1285-x.

Gerlitz, L., Bechtel, B., Böhner, J., Bobrowski, M., Bürzle, B., Müller, M., Scholten, T., Schickhoff, U., Schwab, N. and Weidinger, J. (2016) Analytic comparison of temperature lapse rates and precipitation gradients in a Himalayan treeline environment: implications for statistical downscaling. In: Singh, R.B.,

Schickhoff, U. and Mal, S. (Eds.) *Climate Change, Glacier Response, and Vegetation Dynamics in the Himalaya: Contributions Toward Future Earth Initiatives*. Cham, Switzerland: Springer International Publishing, pp. 49–64. https://doi.org/10.1007/978-3-319-28977-9_3.

Gerlitz, L., Conrad, O. and Böhner, J. (2015) Large-scale atmospheric forcing and topographic modification of precipitation rates over high Asia—a neural-network-based approach. *Earth System Dynamics*, 6(1), 61–81. https://doi.org/10.5194/esd-6-61-2015.

Hasson, S. (2016) Seasonality of precipitation over Himalayan watersheds in CORDEX South Asia and their driving CMIP5 experiments. *Atmosphere*, 7(10), 123.

Hasson, S., Böhner, J. and Chishtie, F. (2018) Low fidelity of CORDEX and their driving experiments indicates future climatic uncertainty over Himalayan watersheds of Indus basin. *Climate Dynamics*, 52, 777–798. https://doi.org/10.1007/s00382-018-4160-0.

Hasson, S., Böhner, J. and Lucarini, V. (2017) Prevailing climatic trends and runoff response from Hindukush–Karakoram–Himalaya, upper Indus Basin. *Earth System Dynamics*, 8, 337–355. https://doi.org/10.5194/esd-8-337-2017.

Hasson, S., Lucarini, V., Pascale, S. and Böhner, J. (2014) Seasonality of the hydrological cycle in major south and southeast Asian river basins as simulated by PCMDI/CMIP3 experiments. *Earth System Dynamics*, 5(1), 67–87. https://doi.org/10.5194/esd-5-67-2014.

Hasson, S., Pascale, S., Lucarini, V. and Böhner, J. (2016) Seasonal cycle of precipitation over major river basins in south and Southeast Asia: a review of the CMIP5 climate models data for present climate and future climate projections. *Atmospheric Research*, 180, 42–63. https://doi.org/10.1016/j.atmosres.2016.05.008.

Hijioka, Y., Lin, E., Pereira, J.J., Corlett, R.T., Cui, X., Insarov, G.E., Lasco, R.D., Lindgren, E. and AS. (2014) IPCC Ch.27 Asia. In: *Climate Change 2014: Impacts, Adaptation, and Vulnerability. Part B: Regional Aspects. Contribution of Working Group II to the Fifth Assessment Report of the Intergovernmental Panel on Climate Change*, pp. 1327–1370. Cambridge: Cambridge University Press. https://doi.org/10.1017/CBO9781107415386.004.

Hingmire, D., Vellore, R.K., Krishnan, R., Ashtikar, N.V., Singh, B.B., Sabade, S. and Madhura, R.K. (2018) Widespread fog over the Indo-Gangetic Plains and possible links to boreal winter teleconnections. *Climate Dynamics*, 52, 5477–5506. https://doi.org/10.1007/s00382-018-4458-y.

IPCC. (2013) *Climate change 2013: the physical science basis. Contribution of Working Group I to the Fifth Assessment Report of the Intergovernmental Panel on Climate Change*. New York: Cambridge University Press, p. 1535. https://doi.org/10.1029/2000JD000115.

Kadel, I., Yamazaki, T. and Iwasaki, T. (2018) Projection of future monsoon precipitation over the Central Himalayas by CMIP5 models under warming scenarios. *Climate Research*, 75(1), 1–21.

Karki, R., Hasson, S., Gerlitz, L., Schickhoff, U., Scholten, T. and Böhner, J. (2017b) Quantifying the added value of convection-permitting climate simulations in complex terrain: a systematic evaluation of WRF over the Himalayas. *Earth System Dynamics*, 8 (3), 507–528. https://doi.org/10.5194/esd-8-507-2017.

Karki, R., Hasson, S., Gerlitz, L., Talchabhadel, R., Schenk, E., Schickhoff, U., Scholten, T. and Böhner, J. (2018) WRF-based simulation of an extreme precipitation event over the Central Himalayas: atmospheric mechanisms and their representation by

microphysics parameterization schemes. *Atmospheric Research*, 214, 21–35. https://doi.org/10.1016/J.ATMOSRES.2018.07.016.

Karki, R., Hasson, S., Schickhoff, U., Scholten, T. and Böhner, J. (2017a) Rising precipitation extremes across Nepal. *Climate*, 5(1), 4. https://doi.org/10.3390/cli5010004.

Karki, R., Talchabhadel, R., Aalto, J. and Baidya, S.K. (2016) New climatic classification of Nepal. *Theoretical and Applied Climatology*, 125(3–4), 799–808. https://doi.org/10.1007/s00704-015-1549-0.

Kattel, D.B. and Yao, T. (2013) Recent temperature trends at mountain stations on the southern slope of the Central Himalayas. *Journal of Earth System Science*, 122(1), 215–227. https://doi.org/10.1007/s12040-012-0257-8.

Kattel, D.B., Yao, T., Yang, K., Tian, L., Yang, G. and Joswiak, D. (2013) Temperature lapse rate in complex mountain terrain on the southern slope of the Central Himalayas. *Theoretical and Applied Climatology*, 113(3–4), 671–682. https://doi.org/10.1007/s00704-012-0816-6.

Kendall, M.G. (1975) *Rank Correlation Method*. London, UK: Griffin.

Khatiwada, K., Panthi, J., Shrestha, M. and Nepal, S. (2016) Hydroclimatic variability in the Karnali River basin of Nepal Himalaya. *Climate*, 4(2), 17. https://doi.org/10.3390/cli4020017.

Klein Tank, A.M.G., Peterson, T.C., Quadir, D.A., Dorji, S., Zou, X., Tang, H., Santhosh, K., Joshi, U.R., Jaswal, A.K., Kolli, R.K., Sikder, A.B., Deshpande, N.R., Revadekar, J.V., Yeleuova, K., Vandasheva, S., Faleyeva, M., Gomboluudev, P., Budhathoki, K.P., Hussain, A., Afzaal, M., Chandrapala, L., Anvar, H., Amanmurad, D., Asanova, V.S., Jones, P.D., New, M.G. and Spektorman, T. (2006) Changes in daily temperature and precipitation extremes in central and South Asia. *Journal of Geophysical Research*, 111(D16), D16105. https://doi.org/10.1029/2005jd006316.

Lang, T.J. and Barros, A.P. (2004) Winter storms in the Central Himalayas. *Journal of the Meteorological Society of Japan*, 82(3), 829–844. https://doi.org/10.2151/jmsj.2004.829.

Mahrt, L. (2006) Variation of surface air temperature in complex terrain. *Journal of Applied Meteorology and Climatology*, 45, 1481–1493. https://doi.org/10.1175/JAM2419.1.

Mainali, J. and Pricope, N.G. (2017) High-resolution spatial assessment of population vulnerability to climate change in Nepal. *Applied Geography*, 82, 66–82. https://doi.org/10.1016/j.apgeog.2017.03.008.

Mann, H.B. (1945) Nonparametric tests against trend. *Econometrica*, 13, 245–259.

Miehe, S., Miehe, G., Miehe, S., Böhner, J., Bäumler, R., Ghimire, S.K., Bhattarai, K., Chaudahry, R.P., Subedi, M., Jha, P.K. and Pendry, C. (2015) Vegetation ecology. In: Miehe, G., Pendry, C.A. and Chaudhary, R.P. (Eds.) *Nepal- An Introduction to the natural history, ecology and human enviroment of the Himalayas*. Edinburgh: Royal Botanic Garden, pp. 385–472.

Minder, J.R., Letcher, T.W. and Liu, C. (2018) The character and causes of elevation-dependent warming in high-resolution simulations of Rocky Mountain climate change. *Journal of Climate*, 31(6), 2093–2113. https://doi.org/10.1175/JCLI-D-17-0321.1.

Minder, J.R., Mote, P.W. and Lundquist, J.D. (2010) Surface temperature lapse rates over complex terrain: lessons from the Cascade Mountains. *Journal of Geophysical Research: Atmospheres*, 115 (14), D14122. https://doi.org/10.1029/2009JD013493.

Nayava, J.L., Adhikary, S. and Bajracharya, O.R. (2017) Spatial and temporal variation of surface air temperature at different altitude zone in recent 30 years over Nepal. *Mausam*, 68(3), 417–428.

Nepal, S. (2016) Impacts of climate change on the hydrological regime of the Koshi river basin in the Himalayan region. *Journal of Hydro-Environment Research*, 10, 76–89. https://doi.org/10.1016/j.jher.2015.12.001.

Norris, J., Carvalho, L.M.V., Jones, C. and Cannon, F. (2015) WRF simulations of two extreme snowfall events associated with contrasting extratropical cyclones over the western and central Himalaya. *Journal of Geophysical Research: Atmospheres*, 120(8), 3114–3138. https://doi.org/10.1002/2014JD022592.

Norris, J., Carvalho, L.M.V., Jones, C. and Cannon, F. (2018) Deciphering the contrasting climatic trends between the central Himalaya and Karakoram with 36 years of WRF simulations. *Climate Dynamics*, 52, 159–180. https://doi.org/10.1007/s00382-018-4133-3.

Norris, J., Carvalho, L.M.V., Jones, C., Cannon, F., Bookhagen, B., Palazzi, E. and Tahir, A.A. (2016) The spatiotemporal variability of precipitation over the Himalaya: evaluation of one-year WRF model simulation. *Climate Dynamics*, 49, 2179–2204. https://doi.org/10.1007/s00382-016-3414-y.

Palazzi, E., Mortarini, L., Terzago, S. and von Hardenberg, J. (2018) Elevation-dependent warming in global climate model simulations at high spatial resolution. *Climate Dynamics*, 52, 2685–2702. https://doi.org/10.1007/s00382-018-4287-z.

Panda, D.K., Mishra, A., Kumar, A., Mandal, K.G., Thakur, A.K. and Srivastava, R.C. (2014) Spatiotemporal patterns in the mean and extreme temperature indices of India, 1971–2005. *International Journal of Climatology*, 34(13), 3585–3603. https://doi.org/10.1002/joc.3931.

Pepin, N., Bradley, R.S., Diaz, H.F., Baraer, M., Caceres, E.B., Forsythe, N., Fowler, H., Greenwood, G., Hashmi, M.Z., Liu, X.D., Miller, J.R., Ning, L., Ohmura, A., Palazzi, E., Rangwala, I., Schöner, W., Severskiy, I., Shahgedanova, M., Wang, M.B., Williamson, S.N. and Yang, D.Q. (2015) Elevation-dependent warming in mountain regions of the world. *Nature Climate Change*, 5, 424–430. https://doi.org/10.1038/nclimate2563.

Qi, W., Zhang, Y., Gao, J., Yang, X., Liu, L. and Khanal, N.R. (2013) Climate change on the southern slope of Mt. Qomolangma (Everest) region in Nepal since 1971. *Journal of Geographical Sciences*, 23(4), 595–611. https://doi.org/10.1007/s11442-013-1031-9.

Revadekar, J.V., Hameed, S., Collins, D., Manton, M., Sheikh, M., Borgaonkar, H.P., Kothawale, D.R., Adnan, M., Ahmed, A.U., Ashraf, J., Baidya, S., Islam, N., Jayasinghearachchi, D., Manzoor, N., Premalal, K.H.M.S. and Shreshta, M.L. (2013) Impact of altitude and latitude on changes in temperature extremes over South Asia during 1971-2000. *International Journal of Climatology*, 33(1), 199–209. https://doi.org/10.1002/joc.3418.

Salerno, F., Guyennon, N., Thakuri, S., Viviano, G., Romano, E., Vuillermoz, E., Cristofanelli, P., Stocchi, P., Agrillo, G., Ma, Y. and Tartari, G. (2015) Weak precipitation, warm winters and springs impact glaciers of south slopes of Mt. Everest (central Himalaya) in the last 2 decades (1994-2013). *The Cryosphere*, 9(3), 1229–1247. https://doi.org/10.5194/tc-9-1229-2015.

Schickhoff, U., Bobrowski, M., Böhner, J., Bürzle, B., Chaudhary, R.P., Gerlitz, L., Lange, J., Müller, M., Scholten, T. and Schwab, N. (2016) Climate change and treeline dynamics in the Himalaya. In: Singh, R.B., Schickhoff, U. and Mal, S. (Eds.) *Climate Change, Glacier Response, and Vegetation Dynamics in the Himalaya: Contributions Toward Future Earth Initiatives*. Cham: Springer International Publishing, pp. 271–306. https://doi.org/10.1007/978-3-319-28977-9_15

Sen, P.K. (1968) Estimates of the regression coefficient based on Kendall's tau. *Journal of the American Statistical Association*, 63 (324), 1379–1389. https://doi.org/10.1080/01621459.1968. 10480934.

Sharma, K.P., Moore, B. and Vorosmarty, C.J. (2000) Anthropogenic, climatic, and hydrologic trends in the Kosi Basin, Himalaya. *Climatic Change*, 47(1), 141–165. https://doi.org/10.1023/A: 1005696808953.

Sheikh, M.M., Manzoor, N., Ashraf, J., Adnan, M., Collins, D., Hameed, S., Manton, M.J., Ahmed, A.U., Baidya, S.K., Borgaonkar, H.P., Islam, N., Jayasinghearachchi, D., Kothawale, D.R., Premalal, K.H.M.S., Revadekar, J.V. and Shrestha, M.L. (2015) Trends in extreme daily rainfall and temperature indices over South Asia. *International Journal of Climatology*, 35(7), 1625–1637. https://doi.org/10.1002/joc.4081.

Shrestha, A.B. and Aryal, R. (2011) Climate change in Nepal and its impact on Himalayan glaciers. *Regional Environmental Change*, 11 (1), 65–77. https://doi.org/10.1007/s10113-010-0174-9.

Shrestha, A.B., Bajracharya, S.R., Sharma, A.R., Duo, C. and Kulkarni, A. (2017) Observed trends and changes in daily temperature and precipitation extremes over the Koshi river basin 1975–2010. *International Journal of Climatology*, 37(2), 1066–1083. https://doi.org/10.1002/joc.4761.

Shrestha, A.B., Wake, C.P., Mayewski, P.A. and Dibb, J.E. (1999) Maximum temperature trends in the Himalaya and its vicinity: an analysis based on temperature records from Nepal for the period 1971-94. *Journal of Climate*, 12(9), 2775–2786. https://doi.org/10. 1175/1520-0442(1999)012<2775:MTTITH>2.0.CO;2.

Shrestha, M.L. (2000) Interannual variation of summer monsoon rainfall over Nepal and its relation to southern oscillation index. *Meteorology and Atmospheric Physics*, 75(1–2), 21–28. https://doi.org/ 10.1007/s007030070012.

Shrestha, S., Moore, G.A. and Peel, M.C. (2018) Trends in winter fog events in the Terai region of Nepal. *Agricultural and Forest Meteorology*, 259, 118–130. https://doi.org/10.1016/j.agrformet.2018. 04.018.

Shrestha, U.B., Gautam, S. and Bawa, K.S. (2012) Widespread climate change in the Himalayas and associated changes in local ecosystems. *PLoS One*, 7(5), e36741. https://doi.org/10.1371/journal. pone.0036741.

Sivakumar, M.V.K. and Stefanski, R. (2011) *Climate change in South Asia BT—climate change and food security in South Asia*. Dordrecht, the Netherlands: Springer, pp. 13–30. https://doi.org/10. 1007/978-90-481-9516-9_2.

Soncini, A., Bocchiola, D., Confortola, G., Minora, U., Vuillermoz, E., Salerno, F., Viviano, G., Shrestha, D., Senese, A., Smiraglia, C. and Diolaiuti, G. (2016) Future hydrological regimes and glacier cover in the Everest region: The casestudy of the upper Dudh Koshi basin. *Science of The Total Environment*, 565, 1084–1101. https://doi.org/10.1016/j.scitotenv.2016.05.138

Syed, F.S., Körnich, H. and Tjernström, M. (2012) On the fog variability over South Asia. *Climate Dynamics*, 39(12), 2993–3005. https://doi.org/10.1007/s00382-012-1414-0.

Talchabhadel, R., Karki, R., Thapa, B.R., Maharjan, M. and Parajuli, B. (2018) Spatio-temporal variability of extreme precipitation in Nepal. *International Journal of Climatology*, 38(11), 4296–4313. https://doi.org/10.1002/joc.5669.

Tong, S., Li, X., Zhang, J., Bao, Y., Bao, Y., Na, L. and Si, A. (2019) Spatial and temporal variability in extreme temperature and precipitation events in Inner Mongolia (China) during 1960–2017. *Science of the Total Environment*, 649, 75–89. https://doi.org/10.1016/j. scitotenv.2018.08.262.

Uddin, K., Shrestha, H.L., Murthy, M.S.R., Bajracharya, B., Shrestha, B., Gilani, H., Pradhan, S. and Dangol, B. (2015) Development of 2010 national land cover database forthe Nepal. *J Environ Manage* 148, 82–90. https://doi.org/10.1016/j.jenvman.2014.07.047

Wang, X.L. (2008) Penalized maximal F test for detecting undocumented mean shift without trend change. *Journal of Atmospheric and Oceanic Technology*, 25(3), 368–384. https://doi.org/10.1175/ 2007JTECHA982.1.

WMO. 2010. *Guide to climatological practices*. Available at: Naturaweb.Net. DOI: https://doi.org/10.11369/jji1950.27.129.

Yue, S., Pilon, P. and Phinney, B.O.B. (2003) Canadian Streamflow Trend Detection : Impacts of Serial and Cross-Correlation. *Hydrological Sciences Journal*, 48, 51–63.

Yue, S. and Wang, C.Y. (2002) Regional streamflow trend detection with consideration of both temporal and spatial correlation. *International Journal of Climatology*, 22(8), 933–946. https://doi.org/10. 1002/joc.781.

SUPPORTING INFORMATION

Additional supporting information may be found online in the Supporting Information section at the end of this article.